

**This document was prepared in conjunction with work accomplished under Contract No. DE-AC09-96SR18500 with the U.S. Department of Energy.**

**This work was prepared under an agreement with and funded by the U.S. Government. Neither the U. S. Government or its employees, nor any of its contractors, subcontractors or their employees, makes any express or implied: 1. warranty or assumes any legal liability for the accuracy, completeness, or for the use or results of such use of any information, product, or process disclosed; or 2. representation that such use or results of such use would not infringe privately owned rights; or 3. endorsement or recommendation of any specifically identified commercial product, process, or service. Any views and opinions of authors expressed in this work do not necessarily state or reflect those of the United States Government, or its contractors, or subcontractors.**

## Control of Nepheline Crystallization in Nuclear Waste Glass WSRC-STI-2006-00379

Kevin M. Fox, Thomas B. Edwards, David K. Peeler  
Savannah River National Laboratory, Aiken, SC 29808, USA

### Abstract

Glass frits with a high  $B_2O_3$  concentration have been designed which, when combined with high-alumina concentration nuclear waste streams, will form glasses with durabilities that are acceptable for repository disposal and predictable using a free energy of hydration model. Two glasses with nepheline discriminator values closest to 0.62 showed significant differences in normalized boron release between the quenched and heat treated versions of each glass. X-ray diffraction confirmed that nepheline crystallized in the glass with the lowest nepheline discriminator value, and nepheline may also exist in the second glass as small nanocrystals. The high- $B_2O_3$  frit was successful in producing simulated waste glasses with no detectable nepheline crystallization at waste loadings of up to 45 wt%. The melt rate of this frit was also considerably better than other frits with increased concentrations of  $Na_2O$ .

### Introduction

High-level wastes, a legacy of Cold War production of nuclear materials for defense, are stored at several Department of Energy (DOE) facilities in the United States. These wastes, typically in the form of a sludge stored in underground tanks, are being vitrified with a glass frit or mined, glass-forming minerals to form a glass wastefrom suitable for final disposal in the national repository. The waste glass must meet DOE requirements for durability, or resistance to chemical leaching in water at elevated temperatures, in order to be acceptable to the repository. A significant volume of these wastes has been identified as containing high concentrations of  $Al_2O_3$  and  $Na_2O$ . Based on current blending and washing strategies, waste streams at the Savannah River Site (SRS) have been identified with  $Al_2O_3$  concentrations from 25 to 40 wt%. Concentrations in some wastes at Hanford are as high as 80 wt%. The combination of high  $Al_2O_3$  and  $Na_2O$  concentrations in the waste, coupled with lower  $SiO_2$  concentrations in the glass as waste loadings (WLs) increase, can lead to the crystallization of nepheline ( $NaAlSi_3O_8$ ). The impact of crystallization, or devitrification, on the durability of the glass wastefrom is dependent upon the type and extent of the crystalline phases that develop.

Several studies have investigated the impacts of crystallization on DOE waste glasses. The formation of spinels ( $MgAl_2O_4$  and others) has been shown to have little or no effect on the durability of some SRS glasses, while the formation of acmite ( $NaFeSi_2O_6$ ) produced a small but noticeable increase in the rate of dissolution of the matrix glass.<sup>1</sup> Kim *et al.* assessed the durability response of over 120 simulated, high-level waste glasses for Hanford as a function of thermal treatment (either quenched or slowly cooled to simulate cooling along the centerline of a stainless steel waste glass container).<sup>2</sup> The results of that study indicated that crystallization, depending on the type and extent, can have an adverse effect on chemical durability. Numerous other studies have assessed the devitrification of high-level waste glass and its potential effect on durability, again with results indicating that the impact of devitrification on durability is dependent on the type and extent of crystallization.<sup>3-6</sup> Several recent reports have shown that nepheline crystallization, even in small amounts, can have a significant, negative impact on the durability of the glass wastefrom.<sup>6-10</sup> Nepheline is therefore of particular concern for vitrification of waste streams with high  $Al_2O_3$  concentrations.

Melt rate, which impacts the efficiency with which the waste can be vitrified, is also a concern for these high  $Al_2O_3$  concentration, nepheline-prone glasses. Based on historical trends at the Defense Waste Processing Facility (DWPF),  $Na_2O$  is usually included in the frit as a flux to enhance melt rate, but the concentrations must be balanced by the  $Na_2O$  concentration in the sludge to ensure product quality. However, the addition of  $Na_2O$  to sludge with a high concentration of  $Al_2O_3$  can increase the propensity for nepheline crystallization in the glass.

The goal of the current study was to formulate a glass frit to be combined with a high- $Al_2O_3$  waste that would provide both a reduced susceptibility to nepheline crystallization and a practical melt rate. Li *et al.* indicated that sodium alumino-borosilicate glasses are prone to nepheline crystallization if their

compositions projected on the  $\text{Na}_2\text{O}-\text{Al}_2\text{O}_3-\text{SiO}_2$  ternary fall within or close to the nepheline primary phase field.<sup>11</sup> In particular, durable glasses with  $\text{SiO}_2/(\text{SiO}_2+\text{Na}_2\text{O}+\text{Al}_2\text{O}_3) > 0.62$ , where the chemical formula stand for the mass fractions in the glass, do not tend to precipitate nepheline as their primary phase.<sup>11</sup> Based on these results, a nepheline discriminator has been incorporated into frit development efforts for SRS wastes.<sup>12</sup>

Li *et al.* also point out that boron has been shown to reduce the propensity for nepheline crystallization by reducing the activity of  $\text{Na}_2\text{O}$  in the melt, and thus preventing it from reacting with aluminum tetrahedra to form nepheline.<sup>11</sup> Based on these results, a glass frit with a relatively high boron concentration was developed for this study and compared with a frit containing a lower boron concentration and a higher  $\text{Na}_2\text{O}$  concentration. Glasses formulated with simulated high- $\text{Al}_2\text{O}_3$  waste and these frits were fabricated and tested in the laboratory.

### **Experimental Procedure**

A series of ten test glass compositions was developed based on the projected composition of a high-alumina nuclear waste sludge to be processed at the DWPF at SRS. A simulated sludge of this composition was combined with a glass frit with a high boron concentration, designated Frit 503, at various WLs to develop the target glass compositions. The composition of Frit 503 is given in Table 1. The two other frits described in this table, Frits 418 and 425, were combined with the simulated sludge for melt rate testing only, which will be described later. Waste loadings were selected that gave glass compositions covering a range of nepheline discriminator values from 0.635 to 0.755 (based on target compositions). The intent was to determine how closely the critical value of 0.62 could be approached before a detectable amount of nepheline would crystallize in the glass upon slow cooling. The target compositions, WLs and nepheline discriminator values are given in Table 2 for the ten study glasses.

Each of the glasses was prepared from the proper proportions of reagent-grade metal oxides, carbonates,  $\text{H}_3\text{BO}_3$ , and salts in 150 g batches. The raw materials for each individual glass were thoroughly mixed and placed into a 95% platinum / 5% gold, 250 ml crucible. The crucible was set in a high-temperature furnace at the melt temperature of 1150°C and held for 1 hour. The glass was poured onto a clean, stainless steel plate and allowed to air cool (quench). The glass pour patty was used as a sampling stock for the various property measurements, including chemical composition and durability. Approximately 25 g of each glass was heat-treated to simulate cooling along the centerline of a DWPF-type canister to gauge the effects of thermal history on the product performance. This cooling schedule is referred to as the canister centerline cooled (ccc) heat treatment.

A representative sample from each glass was characterized to confirm that the as-fabricated glass met the target compositions. Two dissolution techniques, sodium peroxide fusion and lithium-metaborate, were used for each specimen. Each glass was prepared in duplicate for each of the two cation dissolution techniques. All of the prepared samples were analyzed twice for each element of interest by Inductively Coupled Plasma – Atomic Emission Spectroscopy (ICP-AES), with the instrumentation being re-calibrated between the duplicate analyses. Glass standards were also intermittently measured to assess the performance of the ICP-AES instrument over the course of these analyses.

Representative samples of select study glasses were analyzed via X-ray diffraction (XRD). Samples were run under conditions providing a detection limit of approximately 0.5 vol%. That is, if crystals (or undissolved solids) were present at 0.5 vol% or greater, the diffractometer would not only be capable of detecting the crystals but would also allow a qualitative determination of the type of crystal(s) present. Otherwise, a characteristically high background devoid of crystalline spectral peaks indicates that the glass product was amorphous, suggesting either a completely amorphous product or that the degree of crystallization was below the detection limit.

The Product Consistency Test (PCT Method A, see ASTM C 1285) was performed in triplicate on each quenched and ccc glass to assess its chemical durability. Also included in the experimental test matrix was the Environmental Assessment (EA) glass,<sup>13</sup> the Approved Reference Material (ARM) glass, and blanks from the sample cleaning batch. Samples were ground, washed, and prepared according to the ASTM procedure. Fifteen milliliters of Type I ASTM water were added to 1.5 g of glass in stainless steel vessels.

The vessels were closed, sealed, and placed in an oven at  $90 \pm 2^\circ\text{C}$  where the samples were maintained at temperature for 7 days. Once cooled, the resulting solutions were sampled, filtered and acidified in preparation for analysis by ICP-AES to determine the concentration of leached species.

A laboratory-scale, slurry-fed melt rate furnace was used to compare the melting behavior of melter feed containing simulated radioactive sludge mixed with three different frits.<sup>14</sup> This furnace is designed to simulate the conditions found in the joule-heated melter at the DWPF at SRS.<sup>15</sup> The frit/sludge slurry is fed into an Inconel 690 crucible which is resistance heated from the bottom and insulated on the sides. The intent is to simulate the large-scale melter, where heat flow is dependent on convection and conduction between the melt pool and the cold cap that develops as slurry is fed into the furnace. A thermocouple is mounted on the bottom of the crucible to monitor the temperature of the melt, which was held at  $1125^\circ\text{C}$ . Resistance heaters are also positioned in the plenum above the crucible, again to simulate the larger scale melter, and are controlled by a separate thermocouple.

Melt rate testing for each of the three frits began by incrementally feeding the slurry into the furnace to develop a cold cap above the melt pool. The automatic slurry feed system was then engaged. The plenum temperature is used to control a slurry feed pump. This pump delivers approximately 100 g of slurry on to the top of the melt pool when the plenum temperature increases to  $750^\circ\text{C}$ . Molten glass is continuously poured from the crucible through an overflow tube as the slurry is melted. The mass of the poured glass is recorded, along with slurry feed rate. The glass pour rate has been found to be more indicative of the melt rate in the DWPF melter than the slurry feed rate<sup>15</sup> and will be used to compare the three frits evaluated in this study. Glass was poured for between 2.5 and 7 hours for each frit, and the average melt rate over this time period was calculated.

### **Results and Discussion**

After fabrication, the chemical composition of each of the glasses was measured using ICP-AES. The target and measured compositions are listed in individual columns for each glass in Table 2. A value for the nepheline discriminator calculated using the measured composition is also given. A review of these data reveals that there were generally no issues in meeting the target composition for each glass. The NiO and  $\text{SO}_3$  concentrations are lower than the target values for all of the glasses, but this will not influence the outcome of the study.

X-ray diffraction was carried out on the ccc versions of each glass since the slowly cooled specimens have a better kinetic opportunity for crystallization. The XRD results are listed in Table 3. Only two of the glasses, WG-01 and WG-02, contained crystalline phases that were identifiable by XRD. Nepheline was identified in glass WG-01. Based upon its measured composition, this glass had a nepheline discriminator value of 0.619 (i.e. very close to or less than the critical value of 0.62) which predicts that nepheline will precipitate as the primary crystalline phase in this glass. Trevorite was identified in both WG-01 and WG-02. However, spinels generally have little effect on the durability of borosilicate waste glass.<sup>1</sup> The other glasses are either amorphous or contained crystalline regions that were too small to be detectable by XRD. Nepheline in particular has been shown to exist as small nanocrystals or nanoclusters,<sup>11</sup> which may be difficult to detect via XRD.

The results of the PCT for each of the study glasses are listed in Table 4. Both quenched and ccc versions of each glass were included in the PCT. The influence of nepheline in reducing durability is typified by a difference in leaching behavior between the quenched and ccc version of a glass. The magnitude of that difference is typically dependent upon the volume fraction of nepheline formed and the resulting change in composition of the residual glass. The leaching behavior was monitored by measuring the normalized concentration of boron released from the glass. This has been shown to be an excellent indicator of the potential for the release of radionuclides from borosilicate waste glass (see ASTM 1285). Glasses WG-01 and WG-02 both show significant increases in the normalized boron release, or a significant decrease in durability, between the quenched and ccc versions of the glasses (see Table 4). This reduction in durability is most likely due to nepheline crystallization in the ccc glasses during the slow cooling cycle. The remaining study glasses show no significant differences in normalized boron release between the quenched and ccc versions of each glass. This, along with the XRD results, indicates that no durability-affecting crystallization took place in these glasses during the slow cooling cycle.

While a measurable decrease in durability occurred for two of the study glasses, their measured durabilities are still acceptable as compared to the benchmark glass used to qualify vitrified high level waste for disposal in the national repository. This benchmark glass, the Environmental Assessment (EA) glass,<sup>13</sup> has a normalized boron release of 16.695 g/L, which is about an order of magnitude greater than any of the glasses fabricated in this study regardless of thermal history.

Due to the duration of the PCT and the inability to remediate a non-acceptable glass, the durability of the glass poured at the DWPF cannot be monitored online. Instead, a free energy of hydration model is used to predict the durability of the glass based on the measured composition of the slurry feed.<sup>16</sup> This model is also applied to test glasses prepared in the laboratory in order to confirm the model's applicability to a new glass composition. Figure 1 shows a plot of the predicted, normalized boron release of the waste glass versus the free energy of hydration,  $\Delta G_p$ . A prediction interval for an individual PCT response at a 95% confidence level is shown. Data points representing each of the study glasses are included, and all fall within the prediction band. Therefore the durability of each of the study glasses, both quenched and ccc, are predictable using the current DWPF models. Note that the  $\Delta G_p$  model is applicable only to amorphous glasses, so it may not apply to glass WG-01 due to the small amount of nepheline crystallization in this glass.

The melt rates of the three frits described in Table 1, combined as a slurry with the simulated high- $\text{Al}_2\text{O}_3$  sludge, were measured using the slurry-fed, laboratory-scale melter. The results of the melt rate testing are listed in Table 5. Frit 503, with a high boron concentration, had an average melt rate approximately 14% faster than the other two higher  $\text{Na}_2\text{O}$  frits. If realized in the DWPF, an increase in melt rate of this scale would represent a significant time and cost savings in waste vitrification operations. Further work is necessary to better elucidate the role of boron in improving the melt rate of these multi-component glasses. A possible mechanism for the enhanced melt rate may be a reduction in B-O coordination as the boron concentration is increased and the alkali concentration is decreased in the glass. As the  $\text{Na}_2\text{O}$  concentration is reduced, the amount of sodium available for charge balancing  $[\text{BO}_{4/2}]^- \text{Na}^+$  units is reduced, increasing the number of  $\text{BO}_{3/2}$  units. This results in less connectivity in the glass structure, reducing viscosity and glass transformation temperature, which could lead to an improved rate of melting.

### **Conclusions**

Glass frits with a high  $\text{B}_2\text{O}_3$  concentration have been designed which, when combined with high-alumina concentration nuclear waste streams at waste loadings of up to 45%, will form glasses with durabilities that are acceptable for repository disposal and predictable using a free energy of hydration model. The use of such frits would allow the DWPF to vitrify high-aluminum concentration waste over a relatively large range of waste loadings and suggests that aluminum solubility in the glass is not an issue for vitrification of SRS high-level wastes (based on current blending strategies). The measured compositions of each of the ten glasses in this study agreed with the target compositions. The two glasses with nepheline discriminator values closest to 0.62 (i.e., where nepheline is predicted to crystallize) showed significant differences in normalized boron release between the quenched and ccc versions of each glass. XRD confirmed that nepheline crystallized in the glass with the lowest nepheline discriminator value, and nepheline may also exist in the second glass as small nanocrystals. These results show that nepheline crystallization in glasses produced using this high- $\text{B}_2\text{O}_3$  frit can indeed be predicted using the nepheline discriminator, and they provide a good basis for inclusion of a nepheline discriminator value of 0.62 in the online process controls at the DWPF.

The melt rate of glass produced with the high- $\text{B}_2\text{O}_3$  frit was considerably better than other frits with increased concentrations of  $\text{Na}_2\text{O}$ . It is proposed that the increase in melt rate is due to a reduction in the coordination of boron and oxygen when the boron concentration is increased and the alkali concentration is reduced. Further work is necessary to evaluate this theory.

Previous reports in the literature have indicated that  $\text{B}_2\text{O}_3$  is also useful in suppressing nepheline crystallization in glass.<sup>6,11</sup> However, it is interesting to note that there is no  $\text{B}_2\text{O}_3$  term in the nepheline discriminator. Further work is now in progress to better discern the role of  $\text{B}_2\text{O}_3$  in suppressing nepheline crystallization. For example, preliminary glass compositions have been developed with  $\text{B}_2\text{O}_3$

concentrations of 18-20 wt%, Al<sub>2</sub>O<sub>3</sub> concentrations of up to 26 wt%, and nepheline discriminator values of 0.40. These glasses do not precipitate nepheline upon slow cooling and have acceptable durabilities.<sup>17</sup> The 0.62 value is therefore likely to be conservative. Further characterization is underway in order to refine the nepheline discriminator to include the effects of B<sub>2</sub>O<sub>3</sub> and allow for vitrification of high-level wastes containing even higher Al<sub>2</sub>O<sub>3</sub> concentrations.

### **Acknowledgements**

The Savannah River National Laboratory is operated for the U.S. Department of Energy by Washington Savannah River Company under Contract No. DE-AC09-96SR18500. The authors express their gratitude to Irene Reamer, Phyllis Workman, David Best and Patricia Toole for fabrication and characterization of the glass specimens and Michael Smith, Michael Stone, Timothy Jones, and Donald Miller for developing and carrying out melt rate testing.

### **References**

1. Bickford, D. F. and C. M. Jantzen, "Devitrification of SRL Defense Waste Glass," *Sci. Basis for Nuclear Waste Management VII*, edited by G. L. McVay. Elsevier, New York, pp. 557-565 (1984).
2. Kim, D. S., D. K. Peeler and P. Hrma, "Effect of Crystallization on the Chemical Durability of Simulated Nuclear Waste Glasses," *Environmental Issues and Waste Management Technologies in the Ceramic and Nuclear Industries*, Vol. 61, pp. 177-185 (1995).
3. Jantzen, C. M., D. F. Bickford, D. G. Karraker and G. G. Wicks, "Time-Temperature-Transformation Kinetics in SRL Waste Glass," pp. 30-38 in *Advances in Ceramics*, Vol. 8, American Ceramic Society, Westerville, OH (1984).
4. Bickford, D. F. and C. M. Jantzen, "Devitrification of Defense Nuclear Waste Glasses: Role of Melt Insolubles," *J. Non-Crystalline Solids*, **84** [1-3] 299-307 (1986).
5. Spilman, D. B., L. L. Hench and D. E. Clark, "Devitrification and Subsequent Effects on the Leach Behavior of a Simulated Borosilicate Nuclear Waste Glass," *Nuclear and Chemical Waste Management*, **6** 107-119 (1986).
6. Li, H., J. D. Vienna, P. Hrma, D. E. Smith and M. J. Schweiger, "Nepheline Precipitation in High-Level Waste Glasses - Compositional Effects and Impact on the Waste Form Acceptability," *Mat. Res. Soc. Proc.*, Vol. 465, pp. 261-268 (1997).
7. Peeler, D. K., T. B. Edwards, I. A. Reamer and R. J. Workman, "Nepheline Formation Study for Sludge Batch 4 (SB4): Phase 1 Experimental Results," *U.S. Department of Energy Report WSRC-TR-2005-00371, Revision 0*, Westinghouse Savannah River Company, Aiken, South Carolina (2005).
8. Peeler, D. K., T. B. Edwards, D. R. Best, I. A. Reamer and R. J. Workman, "Nepheline Formation Study for Sludge Batch 4 (SB4): Phase 2 Experimental Results," *U.S. Department of Energy Report WSRC-TR-2006-00006, Revision 0*, Washington Savannah River Company, Aiken, South Carolina (2006).
9. Fox, K. M., D. K. Peeler, T. B. Edwards, D. R. Best, I. A. Reamer and R. J. Workman, "Nepheline Formation Study for Sludge Batch 4 (SB4): Phase 3 Experimental Results," *U.S. Department of Energy Report WSRC-TR-2006-00093, Revision 0*, Washington Savannah River Company, Aiken, South Carolina (2006).
10. Fox, K. M., T. B. Edwards, D. K. Peeler, D. R. Best, I. A. Reamer and R. J. Workman, "Durability and Nepheline Crystallization Study for High Level Waste (HLW) Sludge Batch 4 (SB4) Glasses Formulated with Frit 503," *U.S. Department of Energy Report WSRC-STI-2006-00009, Revision 0*, Washington Savannah River Company, Aiken, South Carolina (2006).

11. Li, H., P. Hrma, J. D. Vienna, M. Qian, Y. Su and D. E. Smith, "Effects of  $\text{Al}_2\text{O}_3$ ,  $\text{B}_2\text{O}_3$ ,  $\text{Na}_2\text{O}$ , and  $\text{SiO}_2$  on Nepheline Formation in Borosilicate Glasses: Chemical and Physical Correlations," *J. Non-Crystalline Solids*, **331** 202-216 (2003).
12. Edwards, T. B., D. K. Peeler and K. M. Fox, "The Nepheline Discriminator: Justification and DWPF PCCS Implementation Details," *U.S. Department of Energy Report WSRC-STI-2006-00014, Revision 0*, Washington Savannah River Company, Aiken, South Carolina (2006).
13. Jantzen, C. M., N. E. Bibler, D. C. Beam, C. L. Crawford and M. A. Pickett, "Characterization of the Defense Waste Processing Facility (DWPF) Environmental Assessment (EA) Glass Standard Reference Material," *U.S. Department of Energy Report WSRC-TR-92-346, Revision 1*, Westinghouse Savannah River Company, Aiken, South Carolina (1993).
14. Smith, M. E., M. E. Stone, T. M. Jones, D. H. Miller and P. R. Burket, "SB4 MRF and SMRF Tests with Frits 418, 425, and 503 (U)," *U.S. Department of Energy Report WSRC-STI-2006-00015, Revision 0*, Washington Savannah River Company, Aiken, South Carolina (2006).
15. Smith, M. E., T. H. Lorier and T. M. Jones, "SMRF and MRF DWPF Melt Rate Testing for SB2/SB3 (Case 6B-250 Canisters)," *U.S. Department of Energy Report WSRC-TR-2003-00466*, Westinghouse Savannah River Company, Aiken, South Carolina (2003).
16. Jantzen, C. M., K. G. Brown, T. B. Edwards and J. B. Pickett, "Method of Determining Glass Durability, THERMO™ (Thermodynamic Hydration Energy MOdel)," *United States Patent #5,846,278* (1998).
17. Fox, K.M. and D.K. Peeler, unpublished results (2007).

**Table 1. Composition of Selected Glass Frits (in wt%).**

Frit ID	B <sub>2</sub> O <sub>3</sub>	Li <sub>2</sub> O	Na <sub>2</sub> O	SiO <sub>2</sub>
418	8	8	8	76
425	8	8	10	74
503	14	8	4	74

**Table 2. Composition of Simulated High-level Waste Test Glasses (in wt% calcined oxides).**

WL	WG-01		WG-02		WG-03		WG-04		WG-05		WG-06		WG-07		WG-08		WG-09		WG-10	
	46	46	45	45	42	42	42	42	40	40	38	38	36	36	34	34	32	32	32	32
Composition	target	meas.	target	meas.	target	meas.	target	meas.	target	meas.	target	meas.	target	meas.	target	meas.	target	meas.	target	meas.
Neph. Disc.	0.635	0.619	0.646	0.644	0.658	0.652	0.662	0.655	0.682	0.674	0.702	0.691	0.713	0.706	0.728	0.716	0.742	0.729	0.755	0.743
Al <sub>2</sub> O <sub>3</sub>	10.98	11.29	11.17	11.32	10.83	11.35	10.43	10.77	8.80	9.13	8.72	9.05	8.94	9.28	7.80	8.22	7.95	8.28	7.04	7.41
B <sub>2</sub> O <sub>3</sub>	7.57	7.59	7.71	8.25	8.13	8.11	8.13	8.17	8.41	8.43	8.69	8.49	8.97	8.93	9.25	9.11	9.53	9.12	9.53	9.69
BaO	0.06	0.05	0.06	0.05	0.06	0.05	0.05	0.04	0.04	0.03	0.05	0.04	0.04	0.03	0.04	0.03	0.04	0.04	0.05	0.04
CaO	1.09	1.09	1.08	0.97	0.88	0.87	0.94	0.99	1.05	1.07	0.85	0.88	0.80	0.85	0.76	0.80	0.80	0.82	0.84	0.87
Ce <sub>2</sub> O <sub>3</sub>	0.07	0.04	0.07	0.05	0.07	0.05	0.06	0.02	0.05	0.04	0.06	0.04	0.05	0.02	0.05	0.03	0.05	0.03	0.06	0.04
Cr <sub>2</sub> O <sub>3</sub>	0.10	0.08	0.10	0.06	0.10	0.09	0.08	0.07	0.07	0.06	0.09	0.07	0.07	0.06	0.07	0.06	0.07	0.08	0.08	0.07
CuO	0.03	0.03	0.03	0.04	0.03	0.03	0.02	0.02	0.02	0.02	0.03	0.02	0.02	0.02	0.02	0.02	0.02	0.02	0.02	0.02
Fe <sub>2</sub> O <sub>3</sub>	12.10	10.70	11.97	11.54	10.17	9.51	10.61	9.51	10.58	9.92	10.40	9.18	9.71	8.65	8.83	7.87	8.09	7.08	9.09	8.66
K <sub>2</sub> O	0.15	0.15	0.15	0.16	0.16	0.17	0.13	0.14	0.11	0.09	0.14	0.06	0.11	0.13	0.10	0.08	0.12	0.09	0.12	0.13
La <sub>2</sub> O <sub>3</sub>	0.05	0.04	0.05	0.04	0.05	0.05	0.04	0.03	0.04	0.03	0.04	0.04	0.04	0.03	0.03	0.03	0.04	0.03	0.04	0.03
Li <sub>2</sub> O	4.32	4.30	4.40	4.44	4.64	4.63	4.64	4.61	4.80	4.75	4.96	4.93	5.12	5.09	5.28	5.30	5.44	5.39	5.44	5.40
MgO	1.15	1.14	1.12	1.06	0.94	0.88	0.99	0.90	0.89	0.78	0.90	0.81	0.85	0.74	0.89	0.85	0.84	0.80	0.71	0.61
MnO	2.50	2.52	2.47	2.55	2.39	2.43	2.34	2.40	2.06	2.04	2.11	2.13	1.90	1.94	1.80	1.84	1.78	1.80	1.82	1.80
Na <sub>2</sub> O	13.02	13.75	12.15	12.39	12.47	12.71	12.34	12.98	12.68	13.14	11.43	12.07	10.69	11.25	11.03	11.74	10.06	10.85	9.74	10.33
NiO	0.71	0.55	0.71	0.61	0.54	0.43	0.71	0.57	0.52	0.40	0.54	0.40	0.51	0.40	0.57	0.46	0.46	0.35	0.58	0.48
PbO	0.04	0.04	0.04	0.04	0.05	0.04	0.04	0.03	0.03	0.03	0.04	0.03	0.03	0.02	0.03	0.02	0.03	0.03	0.03	0.03
SiO <sub>2</sub>	41.84	40.75	42.59	42.95	44.74	45.14	44.58	45.09	46.14	46.10	47.39	47.23	48.88	49.26	50.28	50.43	51.68	51.34	51.72	51.29
SO <sub>3</sub>	0.53	0.49	0.50	0.45	0.44	0.37	0.47	0.39	0.42	0.33	0.46	0.36	0.44	0.34	0.41	0.35	0.39	0.34	0.40	0.32
ThO <sub>2</sub>	0.03	0.17	0.03	0.10	0.03	0.14	0.02	0.14	0.02	0.14	0.03	0.13	0.02	0.08	0.02	0.11	0.02	0.09	0.02	0.06
TiO <sub>2</sub>	0.01	0.02	0.01	0.01	0.01	0.02	0.01	0.01	0.01	0.01	0.01	0.01	0.01	0.01	0.01	0.01	0.01	0.01	0.01	0.01
U <sub>3</sub> O <sub>8</sub>	3.50	3.27	3.44	3.28	3.07	2.93	3.25	3.09	3.16	2.98	2.94	2.69	2.69	2.54	2.63	2.46	2.48	2.29	2.52	2.42
ZnO	0.05	0.09	0.04	0.07	0.05	0.05	0.04	0.04	0.03	0.03	0.04	0.04	0.03	0.03	0.03	0.03	0.03	0.03	0.04	0.03
ZrO <sub>2</sub>	0.11	0.10	0.11	0.09	0.12	0.11	0.09	0.08	0.08	0.07	0.10	0.09	0.08	0.06	0.07	0.06	0.08	0.07	0.09	0.08
Sum	100.00	98.24	100.00	100.55	100.00	100.13	100.00	100.08	100.00	99.62	100.00	98.78	100.00	99.79	100.00	99.94	100.00	98.98	100.00	99.80



**Table 3. Crystalline Phases Identified by XRD.**

<b>Glass ID</b>	<b>XRD Results</b>
WG-01	nepheline, trevorite
WG-02	trevorite
WG-03	amorphous
WG-04	amorphous
WG-05	amorphous
WG-06	amorphous
WG-07	amorphous
WG-08	amorphous
WG-09	amorphous
WG-10	amorphous

**Table 4. Product Consistency Test Results Based on Measured Compositions.**

<b>Glass ID</b>	<b>Nepheline Discriminator</b>	<b>Heat Treatment</b>	<b>Normalized Released for Boron (g/L)</b>
WG-01	0.619	quenched ccc	0.78 1.68
WG-02	0.644	quenched ccc	0.73 1.20
WG-03	0.652	quenched ccc	0.65 0.67
WG-04	0.655	quenched ccc	0.73 0.72
WG-05	0.674	quenched ccc	0.73 0.71
WG-06	0.691	quenched ccc	0.72 0.72
WG-07	0.706	quenched ccc	0.60 0.61
WG-08	0.716	quenched ccc	0.67 0.64
WG-09	0.729	quenched ccc	0.63 0.61
WG-10	0.743	quenched ccc	0.61 0.62

**Table 5. Results of Slurry-fed Melt Rate Testing.**

<b>Frit ID</b>	<b>Average Melt Rate (g / minute)</b>
418	11.5
425	11.6
503	13.1

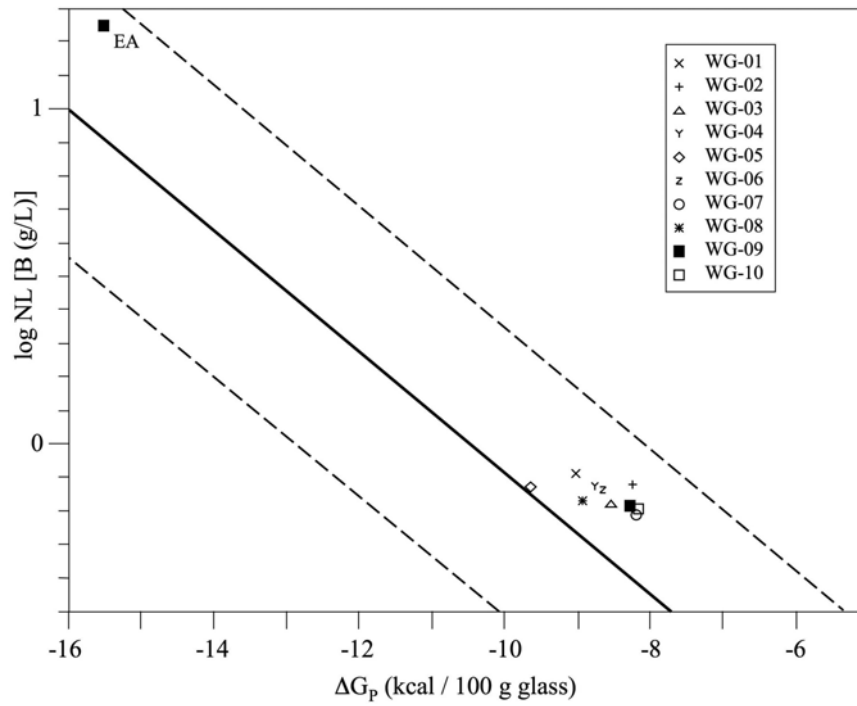


**Figure 1. Predicted, normalized boron release using the free energy of hydration model.<sup>16</sup> Confidence bands at the 95% interval are indicated by the dashed lines. Measured data for the study glasses, indicated by points on the plot, fall within the predicted interval.**